Hindawi
Geofluids
Volume 2022, Article ID 6877500, 14 pages
https://doi.org/10.1155/2022/6877500

*Research Article*

# Petrophysical Characterization and Gas Accumulation of Wufeng-Longmaxi Shale Reservoir in Eastern Margin of Sichuan Basin, SW China

**Wei Wang,[1,2] Dahua Li,[1,2] Lijun Cheng,[1,2] Ye Zhang,[1,2] Jinxi Wang,[1,2] Zhiping Zhang,[1,2] Hualian Zhang,[1,2] Dongxin Guo,[1,2] Yuelei Zhang,[1,2] Qing Hua,[3] and Jun Liu[1,2,4]**

[1]*National and Local Joint Engineering Research Center of Shale Gas Exploration and Development (Chongqing Institute of Geology and Mineral Resources), Chongqing, China*
[2]*Key Laboratory of Shale Gas Exploration, Ministry of Natural Resources (Chongqing Institute of Geology and Mineral Resources), Chongqing, China*
[3]*PetroChina Southwest Oil & Gasfield Company, Chongqing, China*
[4]*MOE Key Laboratory of Deep Earth Science and Engineering, Institute of New Energy and Low-Carbon Technology, Sichuan University, Chengdu, China*

Correspondence should be addressed to Jun Liu; j.liu@scu.edu.cn

Received 8 November 2021; Accepted 27 March 2022; Published 23 May 2022

Academic Editor: Fazhi Yan



Shale gas plays a significant role in meeting the increasing demand of energy resources, which enables the exploration and exploitation of gas from shale reservoir to be emphasized gradually. Aiming to serve a more responsible and efficient shale gas development, for example, to guide the hydraulic/nonaqueous fracturing operation, this work organized a comprehensive assessment on the petrophysical characterization and gas accumulation of the Upper Ordovician Wufeng-Lower Silurian Longmaxi shale reservoir (abbreviated as WL shale). Results indicate that the WL shale in Well-YC4 contains three third-order sequences (SS1-lower WL, SS2-middle WL, and SS3-upper WL), and each sequence contains a transgressive system tract (TST) and a high-stand system tract (HST), according to the logging information. Meanwhile, the SS1, SS2, and SS3 experienced variable sedimentary environment—with different relatively oxygenic and hydrodynamics. And the bottom section (SS1 and SS2) has a soft great brittle index (BI) value than the upper section (SS3), suggesting the bottom WL shale is better suited for hydraulic fracturing than the upper section. Besides, the organic matter indicates the WL shale has a decent hydrocarbon generation ability, and the thermal evolution degree is also conducive to the full generation of shale gas. The gas content of WL shale ranges in the scope of 0.76 $m^3$/t~2.38 $m^3$/t, in which $CH_4$ is the primary composition and occupies 95.51%~99.36%, and the content of heavy hydrocarbon gases is limited. Besides, the drying coefficient indicates the dry gas is the dominate molecular composition in the gas content of WL shale. Hopefully, this work is instructive to a certain extent for the researchers and engineers who are working on WL shale gas in Sichuan basin.

## 1. Introduction

Developing and utilizing clean energy is currently the most practicable measure to combat climate change and to meet ever-increasing energy demand, of which shale gas is expected to be, at the least, one of the eco-friendly energy suppliers from the underground geological resources [1–7]. Against this background, the exploration of shale gas is a revolution and is changing global energy picture all over the world [8–13]. Shale gas is one of the main helpers to enable the American to be an energy exporter now, although the American had the role of being an energy importer for many years [14]. Accordingly, the American does not need much Canadian oil and gas anymore, resulted in that Canada has to turn to Asia, especially to China, to export its energy. In this context, China has achieved the commercial

extraction of gas from shale reservoir, aiming to help to improve the Chinese energy structure that is heavily dependent on coal currently [8, 15, 16]. In China, the shale gas exploration covers most of the national region and involves the shale reservoir from different sedimentary environments, including marine shale, continental shale, and transitional shale. However, for China, the commercial development mainly occurs to the marine shale, especially the Upper Ordovician Wufeng-Lower Silurian Longmaxi shale reservoir (abbreviated as WL shale) in the southern and southeastern Sichuan basin, SW China [9, 17–23].

Unfortunately, even though China has the world's largest deposit of shale gas with estimated recoverable resources of up to 36.1 trillion cubic meters, the current commercial shale gas production in China is far below that in American [24]. Therefore, more scientific deep investigations on the shale-related fields are required for a better development of shale gas in China. Therein, geological assessment for exploration and engineering operation (like the hydraulic/nonaqueous fracturing operation) for extraction are two primary fields in the process of shale gas development; the former one is set to figure out the situation of shale gas resources, while the latter one aims to enable a cost-effective gas extraction based on the geological information [25–29]. During the geological exploration of shale gas, the petrophysical characterization and gas content assessment are indispensable, making it clear that if the shale gas resources are promising or not.

To facilitate the responsible shale gas development in China, especially in Sichuan basin, many sound achievements are made from the perspective of geological exploration. The reservoir characteristics of three typical marine shales in Sichuan basin were compared, by which the advantage and disadvantage of Wufeng shale, Longmaxi shale, and lower Cambrian Niutitang shale for shale gas accumulation were explored [30]. According to the analyses about the sedimentary environment, material basis, storage space, fracability, and reservoir evolution data, the reservoir characteristics of the WL shale, the depth of 2200~4000 m was treated as the favorable section in Sichuan basin and its periphery [31]. Besides, the heterogeneities both in vertical and in horizontal are widely recognized and occur to the reservoir properties of WL shale, such as mineral composition, gas content, and brittle index (BI) [3, 26, 32, 33]. Despite that a number of attentions have been paid to the WL shale in/around Sichuan basin, the current shale gas production related to WL shale are still dissatisfactory, compared to the vast verified reserves exploitable in this target formation [34, 35]. This indicates that more investigations are needed to push the development of shale gas in/around Sichuan basin, in which the WL shale is of primary importance because it is generally considered as the most promising geological formation.

Recently, an exploration well of shale gas, labelled as Well-YC4, was implemented in the eastern margin of Sichuan basin, offering a rare opportunity to investigate the WL shale, in a comprehensive manner. By this chance, the well drilling, well logging, and laboratorial work together form a systematic scientific structure, aiming at clarifying the shale gas potential in this area. In the area that Well-YC4 locates at, few gas wells are deployed before, so the information from Well-YC4 is precious and is of significance. In this work, the petrophysical characterization and gas accumulation of WL shale are discussed, according to the detailed information from Well-YC4. Hopefully, this work is helpful in deepening the knowledge on the resource potential of shale gas and in guiding the further arrangement of shale gas exploration in the eastern margin of Sichuan basin, such as the resource evaluation, the hydraulic fracturing, and even, the nonaqueous fracturing (e.g., liquid/supercritical $CO_2$ fracturing).

## 2. Geological Background

In this work, the involved shale gas well, Well-YC4, is located at the Wulong County, a city in eastern Chongqing municipality, that is, in geographical, ~150 km far away from Chongqing urban. Geologically, the tectonic environment is regarded as complicated and is mainly composed of a series of S-N and NE-SW trending fault zones and fold belts [36–40]. The current complicated geological setting related to this work, like numerous faults (some now active), universally steep dips, and high tectonic stress, is the composite outcomes resulted from the multiple stages of tectonic activity, including the Caledonian orogeny (542–386 Ma), Hercynian orogeny (386–257 Ma), Indo-China movement (257–205 Ma), Yanshan movement (205–65 Ma), and Himalayan orogeny (beginning 65 Ma) [30, 41]. Therein, the Caledonian movement enabled the stratigraphic lacuna of the Devonian and Carboniferous systems, except from the Neoproterozoic Sinian, Paleozoic, and Mesozoic systems in this involved area [41–43]. Nowadays, four sets of hydrocarbon source rocks exist in study area, namely, the lower Cambrian Niutitang shale, the WL shale, the lower Permian carbonate source rocks, and the upper Permian coal-bearing shale [30, 43–45]. Among these sedimentary strata, the WL shale is the targeted strata of Well-YC4 and is the research object of this work.

In the southeastern Sichuan basin, the WL shale has a thickness ranging from 35 m to 200 m and a maximum burial depth of 4900 m (Figure 1) [46]. As for the Well-YC4, the well depth is ~800 m, and it met seven sets of strata in total, which from the top to the bottom consists of Quaternary, Silurian Xiaoheba formation, Silurian Xintan formation, Silurian Longmaxi formation, Ordovician Wufeng formation, Ordovician Linxiang formation, and Ordovician Baota formation. The basic information of each involved stratum is exhibited in Table 1, in which the targeted WL shale, the combination of Ordovician Wufeng formation and Silurian Longmaxi formation, has a thickness of 118 m in total.

## 3. Materials and Analytical Methodology

Collected from the Well-YC4, in total of 54 shale samples were involved for the investigation of this work. In this work, the petrophysical properties mainly contain the petrologic characteristic and the pore system characterization. Herein,

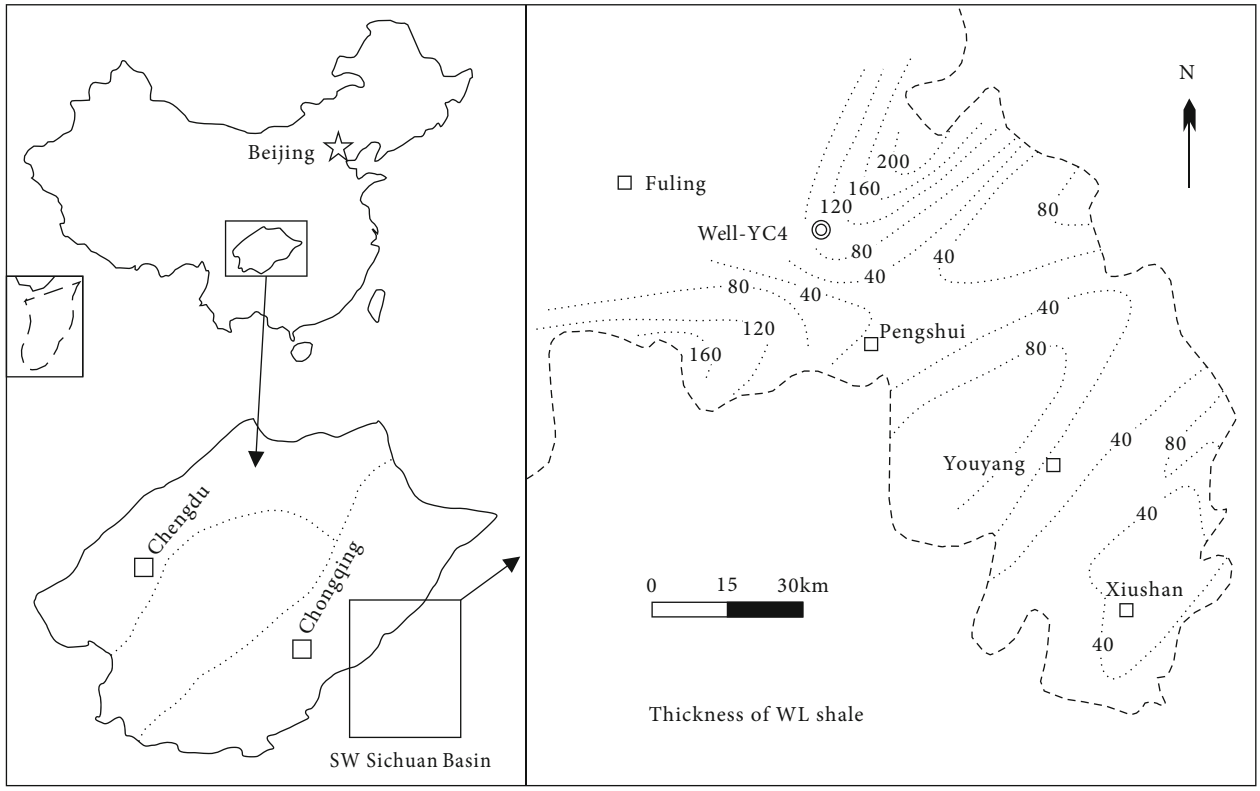


Figure 1: Regional overview of the Well-YC4 and its surrounding area [30, 36, 46].

Table 1: Brief information of the drilled strata in Well-YC4.

| System | Formation | Thickness (m) | Petrographic description |
|---|---|---|---|
| Quaternary | | 6.5 | Topsoil, mainly composed of sandy mudstone, sandstone, and limestone |
| Silurian | Xiaoheba | 132.7 | Greenish-gray shales, gray siltstones, deep to dark gray argillaceous siltstones with silty bands |
| | Xintan | 505.8 | The upper section is grayish to greenish gray argillaceous siltstone and gray argillaceous siltstone, while the lower section is greenish gray silty shale, dark gray silty shale and greenish gray shale, with horizontal bedding. |
| | Longmaxi | 109.6 | Dark gray shale, black carbonaceous shale, and black-gray carbonaceous silty shale, which contains graptolite and occasional patches of pyrite. |
| Ordovician | Wufeng | 8.4 | Dark grey silty shale with horizontal bedding, carbonaceous shale bands, pyrite bearing nodules, and graptolite bearing. |
| | Linxiang | 12.4 | Gray nodular argillaceous limestone |
| | Baota | 25.6 | Dark gray turtle crack limestone with turtle crack structure |

the X-ray diffraction (XRD) was introduced to investigate the mineral composition, and the low-pressure $N_2$ adsorption experiment and scanning electron microscopy were employed for the characterization of pore system in shale. Besides, the onsite desorbed gases from the desorption canisters were used to analyze the gas content and molecular components. The gas molecular components were analyzed using a gas chromatograph equipped with a flame ionization detector and a thermal conductivity detector, and subsequently corrected for the bulk compositional analyses of oxygen. Besides, the scanning electron microscope (SEM) imaging is also used in this work, aiming to observe the pore system in the collected samples in a direct manner. In addition, the total organic carbon (TOC) and vitrinite reflectance ($R_o$) were also measured for the comprehensive study in this work. The detailed operations regarding the above-mentioned methodologies are exhibited in previous works [26, 30, 46–48].

## 4. Results and Discussion

*4.1. Sedimentary Characteristics and Sequence Stratigraphy.* In the Well-YC4, the buried depth of WL shale is 645 m~763 m, where the thickness of Longmaxi shale and Wufeng shale is 109.6 m and 8.4 m, respectively. The stratigraphic division is a comprehensive result from the core observation and logging information. As for the bottom of WL shale, the logging results experienced abrupt changes

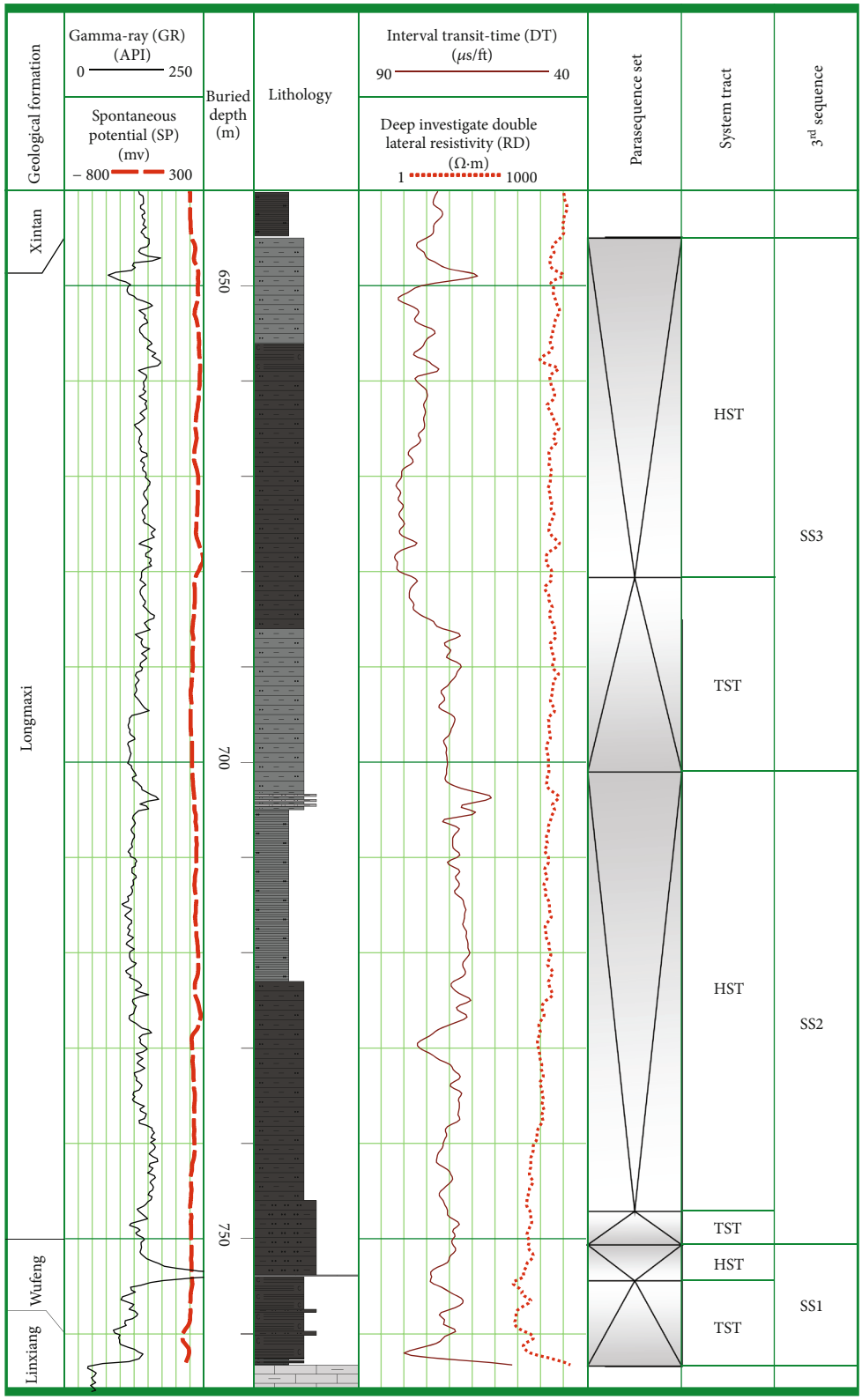


Figure 2: Stratigraphic correlation diagram and vertical variations in the sedimentary sequence of the WL shale in Well-YC4. TST: transgressive system tract; HST: high-stand system tract.

at the boundary between Wufeng formation and Linxiang formation (Figure 2). Herein, the gamma-ray (GR) value for the Wufeng formation is regarded as high and is generally greater than 138 API, while that for Linxiang formation is basically lower than 50 API. The interval transit-time (DT) curve also has an abrupt change, in which the DT value

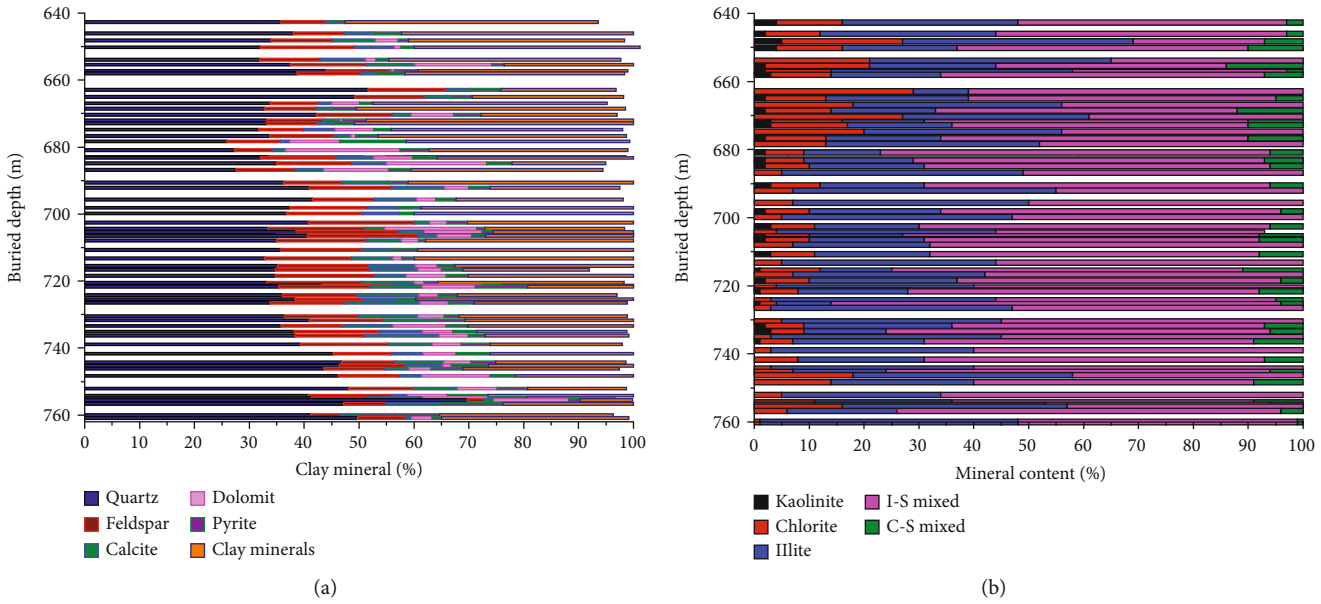


Figure 3: Mineral composition (a) and clay mineral analysis (b) of shale samples from Well-YC4. I-S: illite-smectite mixed-layer mineral; C-S: chlorit -smectite mixed-layer mineral.

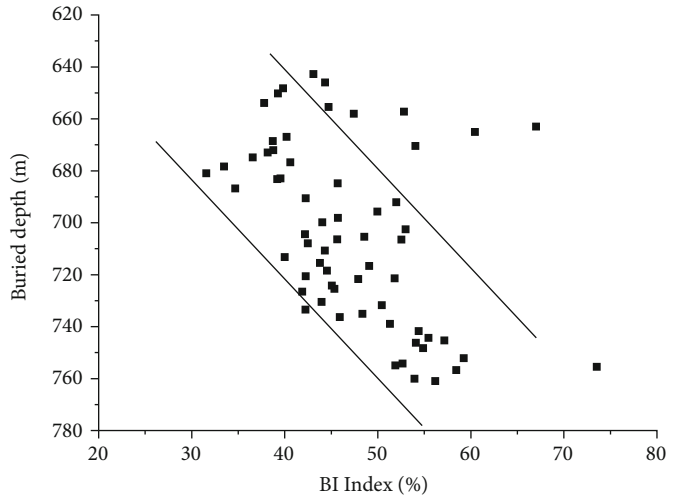


Figure 4: Vertical variation of BI value for the WL shale in Well-YC4.

for the Wufeng formation is overall greater than 74 $\mu$s/ft and that for Lingxiang formation is lower than 52 $\mu$s/ft. Besides, abrupt change also occurs to the spontaneous potential (SP) and deeply investigates double-lateral resistivity (RD) curves at the contact surface between Wufeng formation and Linxiang formation (Figure 2). In the roof of WL shale, logging information also has some abrupt changes, which is treated as the sign of the boundary between Longmaxi formation and Xintan formation, and the related curves are exhibited in Figure 2.

According to the core observation and logging information, the two sequence boundaries in the WL shale were identified; accordingly, the sequence stratigraphic framework of Well-YC4 in the WL shale was established (Figure 2). The two sequence boundaries are manifested as a flooding surface, which divide the WL shale of Well-YC4 into three third-order sequences (SS1, SS2, and SS3) from the lower section to the upper section (Figure 2). Herein, each sequence is composed of a transgressive system tract (TST) and a high-stand system tract (HST) according to the vertical variation in GR logging. This sequence division is consistent with previous works, such as the investigations based on the shale gas wells of Well-JY1, Well-PY1, and Well-WQ2 [26, 46, 49–51], indicating the reliability of this work and the general law for sequence division in WL shale from Sichuan basin and its peripheral areas. Basically, the TST and HST in each third-order sequence correspond to variable formation thickness, where the SS1 is recognized at Wufeng formation, while the SS2 and SS3 are the lower section and upper section of Longmaxi formation, respectively (Figure 2). Regarding each third-order sequence, the TST exhibits an upward increasing trend, while the HST

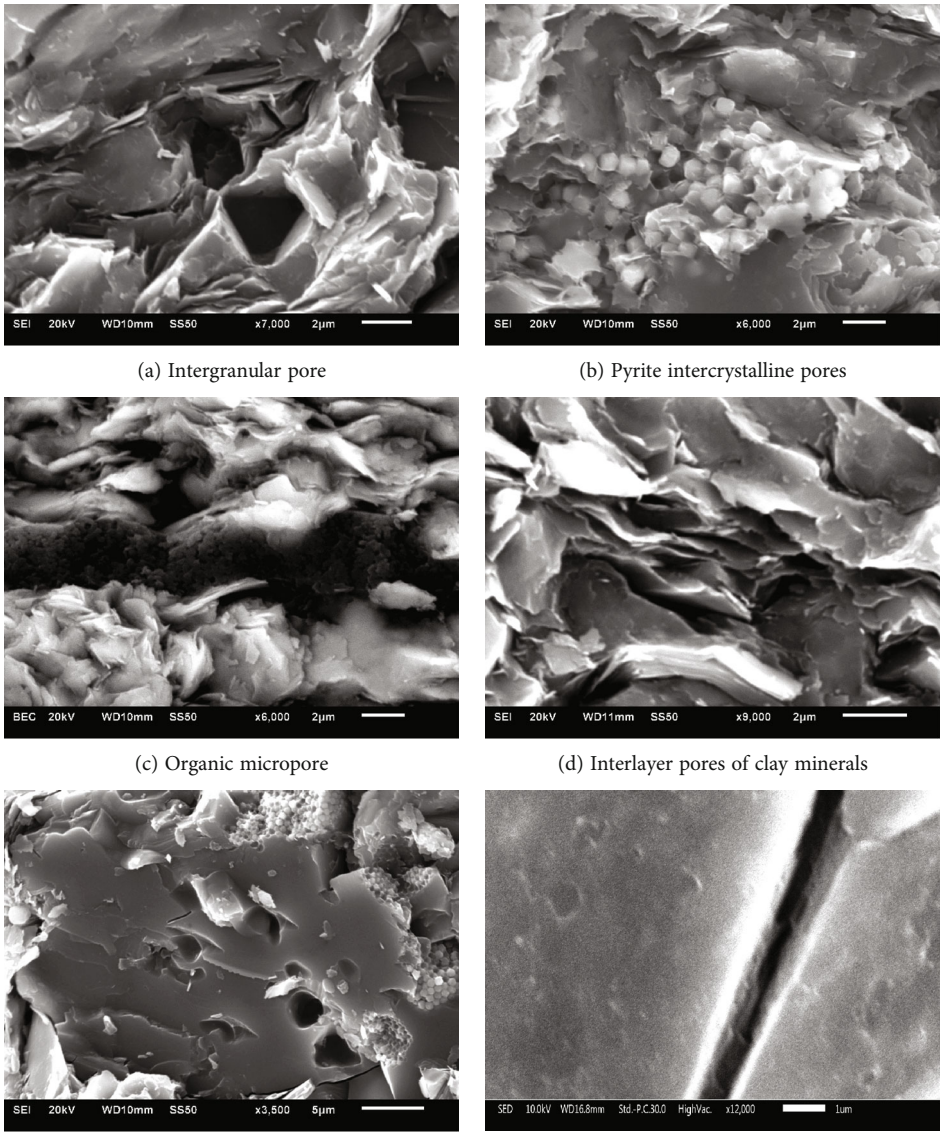


(a) Intergranular pore

(b) Pyrite intercrystalline pores

(c) Organic micropore

(d) Interlayer pores of clay minerals

(e) Intragranular pore

(f) Microfracture

Figure 5: Pore system classification for WL shale of Well-YC4.

displays an upward decreasing trend based on the GR response. Besides, according to the core observation, the amount and species of graptolites exhibit upward decreasing trends, indicating that the water depth was much deeper in the early phase of the deposition (SS1 and SS2) than in the late phase (SS3) [26, 49]. Meanwhile, as for SS1, SS2, and SS3, the sedimentary environment differs from each other—with different relatively oxygenic and hydrodynamics; in the upper WL shale, namely, SS3, the sediment sources seem to contain more terrigenous sand and silty materials, compared to the situation of SS1 and SS2 (Figure 2).

### 4.2. Reservoir Characterization

*4.2.1. Mineral Composition.* The mineralogical analyses of the WL shale are presented in Figure 3. The mineralogy of all collected samples is dominated by quartz and clay minerals, followed by the feldspars, carbonates (dolomite and calcite), and pyrite. Herein, the average content of quartz and clay minerals is 38.3% and 32.3%, respectively, for the WL shale of Well-YC4 (Figure 3(a)). In general, the mineral composition can reflect the shale brittleness—a key factor in promoting hydraulic fracturing as a stimulation method. Meanwhile, the BI index is commonly used to represent the brittleness, which is treated as a key parameter in the evaluation of gas reservoirs. According to the mineral composition, the BI is calculated as follows [52]:

$$\mathrm{BI} = \frac{Q}{(Q + c + Cly)} \times 100\%, \tag{1}$$

where BI is the brittleness index and $Q$, $C$, and $Cly$ represent the contents of quartz, carbonate minerals, and clay minerals, respectively.

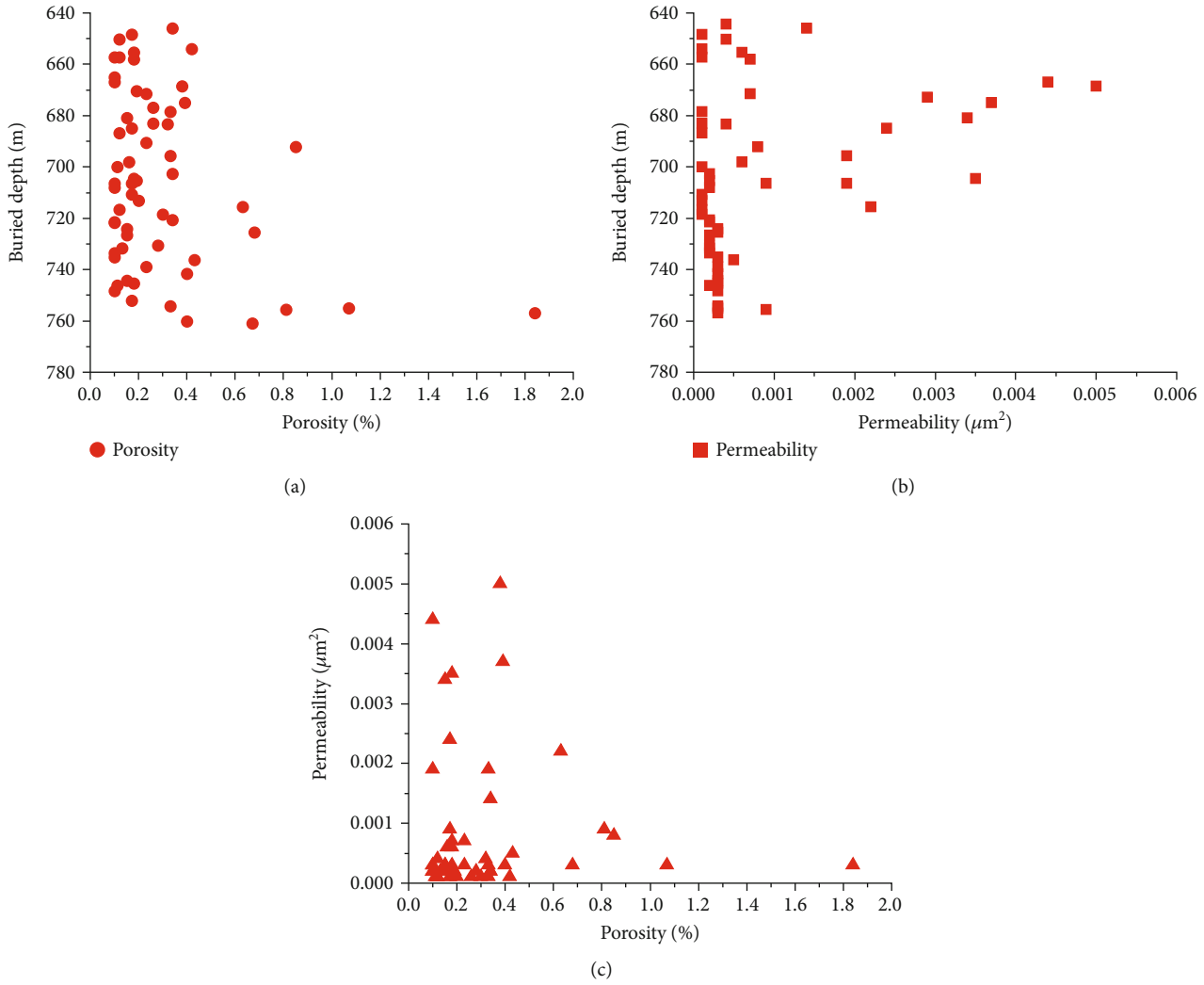


Figure 6: Effective porosity (a), permeability (b), and their relationship (c) of WL shale with different buried depth in Well-YC4.

Based on Equation (1), the calculated results of BI for the WL shale of Well-YC4 are shown in Figure 4, exhibiting a BI value scope of 31.6%~73.5% with an average of 47%. By comparison, in vertical, the bottom section (SS1 and SS2) has a soft great BI value than the upper section (SS3). This phenomenon indicates the bottom WL shale is better suited for hydraulic fracturing than the upper section. This phenomenon keeps pace with the investigation on the Well-WQ2, a shale gas well targeted at WL shale in the northeastern Sichuan basin [26].

Clay minerals are a complex group and mainly contain illite and illite-smectite mixed-layer mineral, supplied with kaolinite, chlorite, and chlorit-smectite mixed-layer mineral (Figure 3(b)). Regarding WL shale, the illite occurs with a percentage of 10-53% and an average 29%, while the illite-smectite mixed-layer mineral ranges from 24% to 82% with an average of 55%. Besides, the content of chlorite varies from 1% to 29% with a mean of 10%. Besides, the illite-smectite mixed-layer ratios of all collected samples locate at 5%~11%, which is characterized as small and suggests a sufficient organic evolution of WL shale [53].

*4.2.2. Pore System Characterization.* In general, shale gas reservoir has a complex type in pore structure and pore size distribution, which has a great influence on the storage and transport mechanism of gas in shales [32, 35, 54–59]. According to the SEM observation, the pore system of WL shale can be divided into six types: intergranular pore, pyrite intercrystalline pores, organic micropore, interlayer pores of clay minerals, intragranular pore, and microfracture (Figure 5). The intergranular pore usually occurs at the silty shale and argillaceous siltstone with heavy sandy content (Figure 5(a)), in which the larger the mineral grain, the larger the intergranular pores. The pyrite intercrystalline pore is always developed at where the pyrite exists (Figure 5(b)), while the organic micropore is related to the organic matter and basically is resulted from the hydrocarbon production (Figure 5(c)). The interlayer pores distribute mainly in the clay minerals which are usually sheet or bedded and thus have free space between layers (Figure 5(d)). The intragranular pore refers to the pores in mineral particles, mainly caused by the dissolution of quartz, calcite, and dolomite and other soluble minerals (Figure 5(e)). These

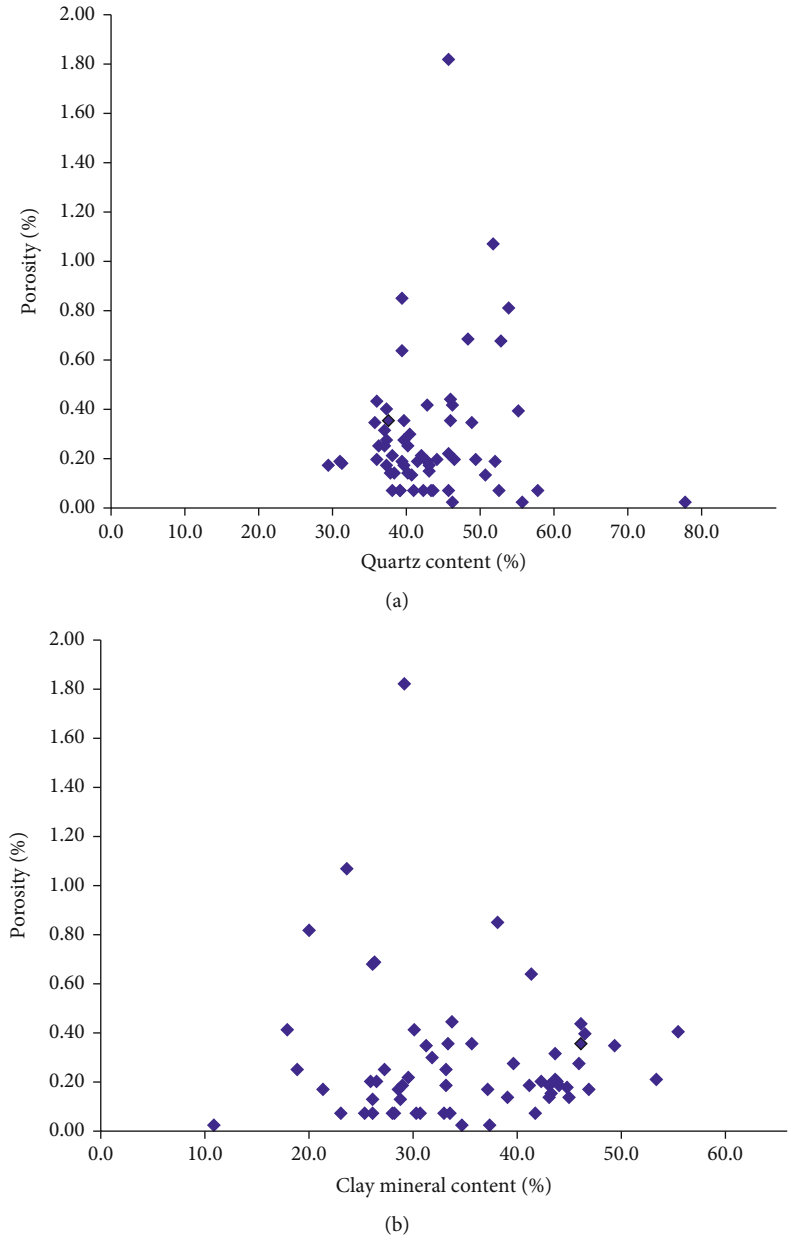


Figure 7: Relationship between porosity and (a) quartz and (b) clay mineral content.

dissolution pores are irregular in shape and developed in groups. Besides, microfracture is also observed in WL shale and is of significance for the gas seepage in shale (Figure 5(e)).

Basically, porosity controls the gas content of shale to a certain extent, and permeability is an important parameter to judge whether a shale gas reservoir has economic value. The effective porosity, permeability, and their relationship are exhibited in Figure 6. Although pore type in WL shale of Well-YC4 is diversiform, the porosity is low, where the highest effective porosity is just 1.84%, and the majority locate in the range of 0.1%~0.4% (Figure 6(a)). According to the scatter diagrams made by the effective porosity and main mineral content (quartz and clay mineral) of WL shale, either the quartz content (Figure 7(a)) or the clay mineral content (Figure 7(b)) insignificantly affects the porosity. As for the permeability, it is mainly within the scope of $0.0001\,\mu m^2$~$0.0044\,\mu m^2$ and has an average of $0.0008\,\mu m^2$ (Figure 6(b)). In vertical, an inconspicuous variation goes to the porosity and permeability, which differs from the vertical heterogeneity observed in another shale gas well (Well-WQ2) located in the northeastern Sichuan basin [26]. Herein, further investigations are needed to clarify this phenomenon, because previous achievements tend to support the heterogeneous porosity and permeability in vertical, regarding the WL shale in Sichuan basin and its peripheral areas [26, 46, 49, 51]. Besides, in this work, the correlation between effective porosity and permeability of WL shale is unobvious (Figure 6(c)), indicating the pores in shale sparingly participate in the seepage behavior of fluids in WL

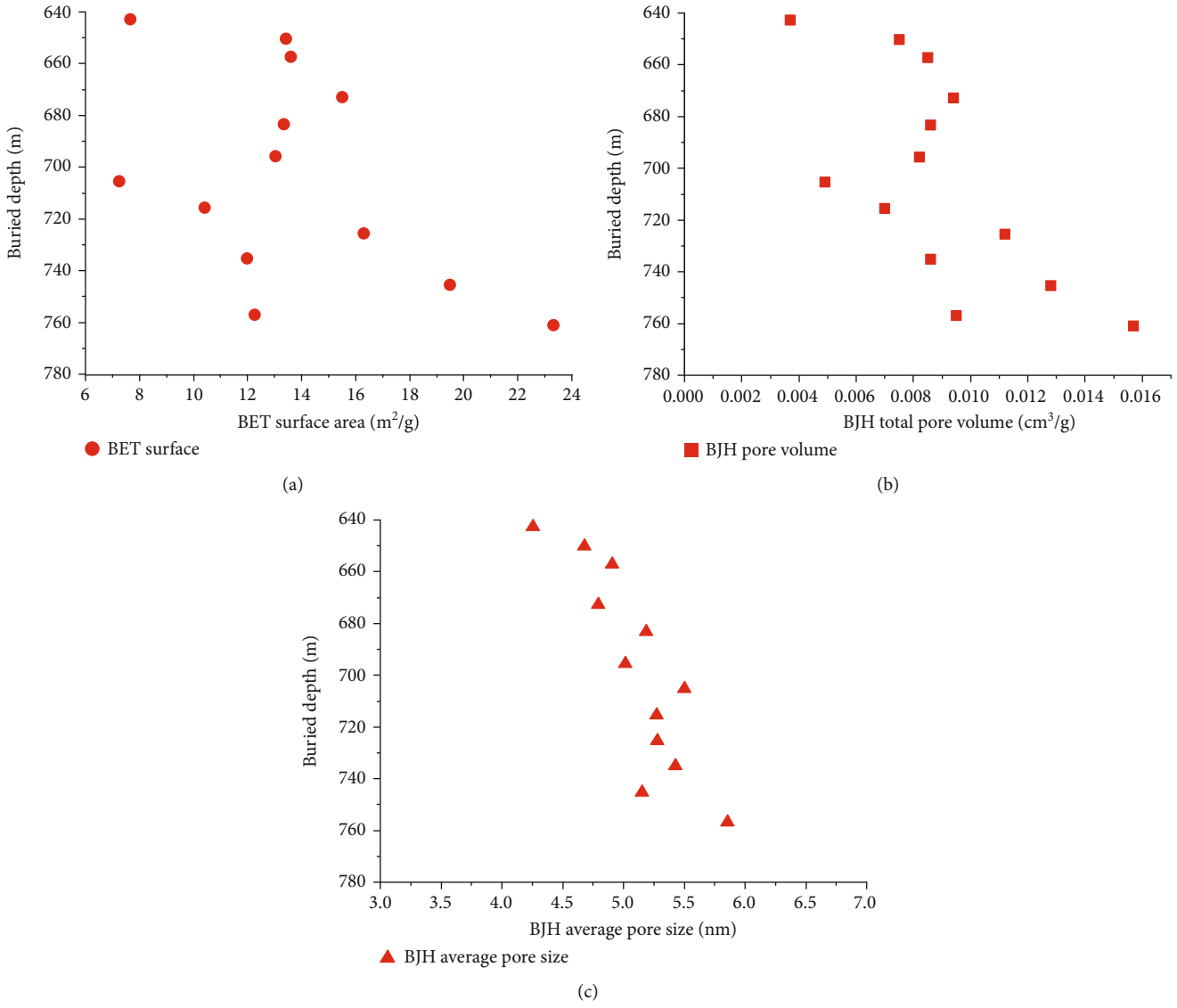


Figure 8: Pore system characterization of collected samples of WL shale in Well-YC4.

reservoir. This phenomenon is unfriendly for an effective gas extraction from WL shale during the potential shale gas development in area nearby Well-YC4. By comparison, the unobvious correlations in this work, regarding porosity and permeability, differ from some other achievements. According to Liu et al. [26], a linear relationship between porosity and permeability was observed in the Longmaxi formation shale, based on the Well-WQ2 in the northeastern Sichuan basin. However, the reason making this inconsistent view between previous acknowledge and this work needs more attentions further.

Besides, the low-pressure $N_2$ adsorption experiments indicate the BET surface area of WL shale in Well-YC4 mainly locates at 7.2344 $m^2/g$~23.3031 $m^2/g$ with an average of 13.6450 $m^2/g$. For the involved samples, over 80% of measured BET surface area is greater than 10 $m^2/g$, suggesting the micropores are well developed (Figure 8(a)). As for the BJH total pore volume, it varies from 0.0037 $cm^3/g$ to 0.0157 $cm^3/g$ with an average of 0.0089 $cm^3/g$ (Figure 8(b)). Herein, the large range for the BET surface area and the BJH total pore volume suggests that a strong heterogeneity in vertical occurs to the pore system of WL shale from Well-YC4. Besides, the BJH average pore size locates at 4.26~5.86 nm and averages 5.12 nm (Figure 8(c)), which is a bit smaller than that (a mean of 6.28 nm) of Longmaxi shale from Jiaoshiba shale gas field, a place nearby the location of Well-YC4 (<100 km in geographical), reported by Liu et al. [17].

*4.2.3. TOC Content and Thermal Maturity.* TOC content usually refers to the percentage of organic carbon of rock mass in the rocks and can approximate representative rocks of original organic matter abundance, which thus is the effective index for the evaluation on the original hydrocarbon generation ability [30, 60, 61]. Overall, the TOC content of WL shale in Well-YC4 is characterized as high. In total, 64 samples are measured, in which the TOC content mainly locates at 1%~5% (~88% of total statistics) (Figure 9(a)). The

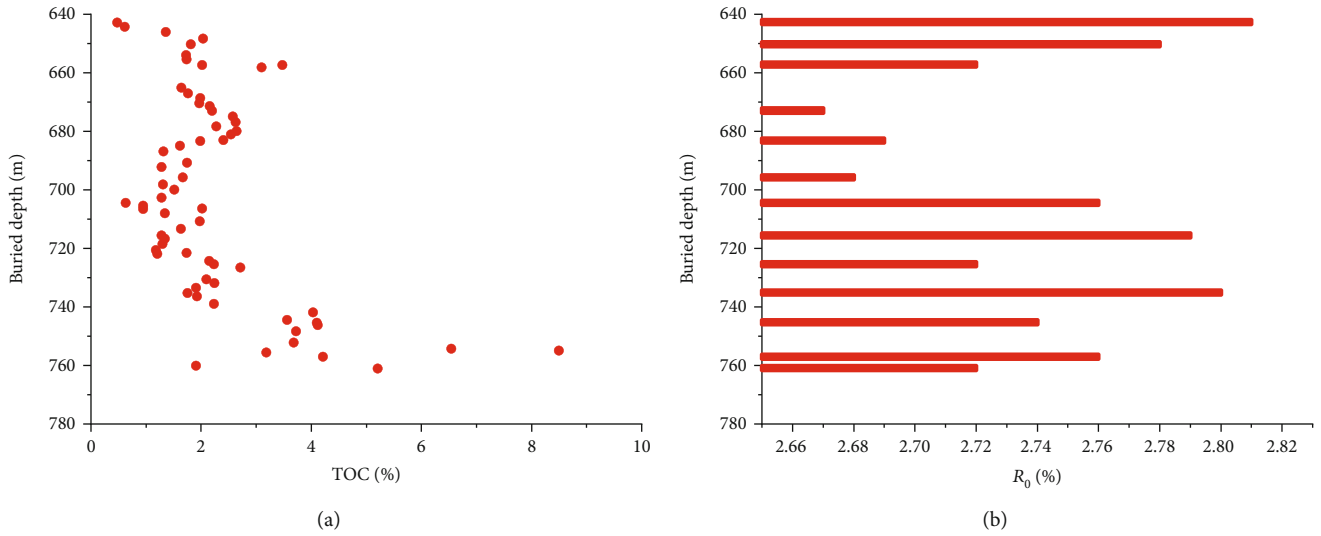


Figure 9: TOC content (a) and $R_o$ value (b) of WL shale in Well-YC4.

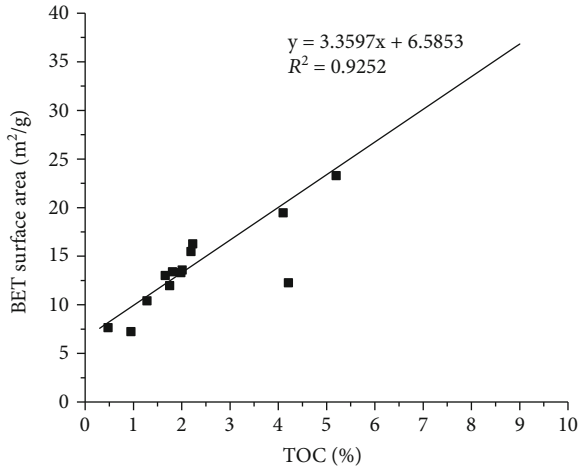


Figure 10: Relationship between the TOC content and BET surface area.

TOC content indicates the WL shale has a decent hydrocarbon generation ability. Herein, the measured values of TOC content exhibit a good linear relationship with BET surface area, as shown in Figure 10, indicating the significant contribution of BET surface area is related to the organic matter. This phenomenon also indicates the organic matter influences a lot on the pore system regarding the WL shale in this work. Besides, the $R_o$ is an internationally recognized independent index for the maturity judgement of organic matter. The measured $R_o$ values locate at 2.68%~2.81% with an average of 2.75%, showing a high thermal evolution process (Figure 9(b)), which works in concert with the small illite-smectite mixed-layer ratios (5%~11%) of WL shale from Well-YC4. This phenomenon indicates that the thermal evolution degree of the WL shale is basically in the early stage of overmature evolution, and the organic matter in shale has reached the peak of gas generation, which is conducive to the full generation of shale gas. In general, the decent hydrocarbon generation ability revealed by TOC content and the sufficient thermal evolution symbolized by $R_o$ together suggest that a mount of hydrocarbon has been generated during the geological period, which is the precondition for the great potential of shale gas development in Sichuan basin.

### 4.3. Gas Accumulation Investigation

*4.3.1. Gas Content.* Herein, three steps were recorded during the coring process, including the beginning of core barrel extraction, when the barrel reached the surface and when the core was placed into the desorption canister, to measure the in situ gas content; thus, the measured total in situ gas content contains desorbed gas, lost gas, and residual gas. This methodology is exhibited in detail by Hartman et al. [62]. The gas content of WL shale is demonstrated in Figure 11, in which the mean is 1.22 $m^3$/t, and the range is 0.76 $m^3$/t~2.38 $m^3$/t. In vertical, the lower section (depth of 724~736 m) has the highest gas content with an average of 1.44 $m^3$/t (0.99 $m^3$/t~2.38 $m^3$/t), while the middle section (685 m~724 m) contains the lowest gas content, and its average is 0.98 $m^3$/t. Besides, as for the upper section (645 m~685 m), the gas content locates at 0.89 $m^3$/t~1.53 $m^3$/t with a mean of 1.24 $m^3$/t. Basically, the gas content varies along with the buried depth in vertical, and the distribution of gas content in vertical is relatively heterogeneous to some extent in the Well-YC4. This phenomenon is consistent with some previous acknowledge on the gas content in WL shale. For example, the vertical heterogeneity of gas content is strong in the WL shale in the wells of Well-PY1 and Well-JY1 located in the southeastern Sichuan basin, where the gas content in the bottom section of WL is the highest and is obviously greater than that in the middle and upper sections, reported by Chen et al. [49]. Accordingly, the bottom section (SS1) is appropriate for the potential deployment of horizontal well during the shale gas extraction, because of the preponderant gas content in the bottom WL shale of Well-YC4 and the greater BI in this section (Figure 4).

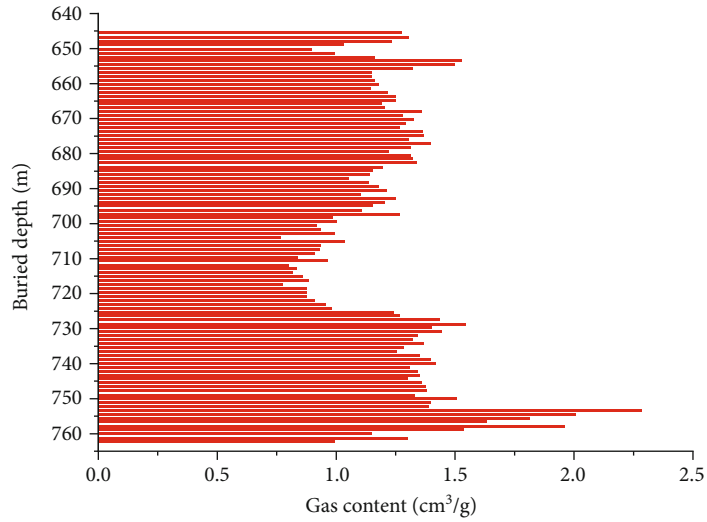


Figure 11: Gas content variation along with the buried depth of WL shale in Well-YC4.

Table 2: Gas molecular composition of WL shale in Well-YC4.

| Sample ID | Depth (m) | $C_1$ (%) | $C_{2+}$ (%) | $C_1$-$C_5$ (%) | Drying coefficient ($C_1$/$C_1$-$C_5$) | $C_{6+}$ (%) | $N_2$ (%) | $CO_2$ (%) |
|---|---|---|---|---|---|---|---|---|
| YC4-4 | 647.2 | 98.51 | 0.59 | 99.10 | 0.99 | 0.53 | 0 | 0.37 |
| YC4-10 | 653.3 | 98.3 | 0.41 | 98.71 | 1.00 | 0.86 | 0 | 0.43 |
| YC4-17 | 658 | 98.5 | 0.63 | 99.13 | 0.99 | 0.45 | 0 | 0.42 |
| YC4-24 | 665 | 97.74 | 0.37 | 98.11 | 1.00 | 1.42 | 0 | 0.47 |
| YC4-31 | 672 | 97.55 | 0.66 | 98.21 | 0.99 | 1.1 | 0 | 0.7 |
| YC4-38 | 678.6 | 98.12 | 0.52 | 98.64 | 0.99 | 0.72 | 0 | 0.64 |
| YC4-45 | 683.9 | 98.37 | 0.81 | 99.18 | 0.99 | 0.65 | 0 | 0.17 |
| YC4-50 | 693 | 98.65 | 0.56 | 99.21 | 0.99 | 0.68 | 0 | 0.12 |
| YC4-58 | 703.6 | 98.66 | 0.482 | 99.14 | 1.00 | 0.61 | 0 | 0.25 |
| YC4-66 | 712.25 | 98.08 | 1.1 | 99.18 | 0.99 | 0.65 | 0 | 0.17 |
| YC4-71 | 718.4 | 98.44 | 0.65 | 99.09 | 0.99 | 0.64 | 0.22 | 0.06 |
| YC4-76 | 724 | 96.68 | 0.68 | 97.36 | 0.99 | 0.68 | 1.08 | 0.17 |
| YC4-82 | 730.5 | 98.87 | 0.39 | 99.26 | 1.00 | / | 0 | 0.74 |
| YC4-87 | 735.4 | 98.91 | 0.77 | 99.68 | 0.99 | / | 0 | 0.32 |
| YC4-92 | 741.7 | 98.5 | 0.81 | 99.31 | 0.99 | / | 0.33 | 0.38 |
| YC4-96 | 746.2 | 97.25 | 0.8 | 98.05 | 0.99 | / | 0.87 | 0.62 |
| YC4-100 | 751.1 | 96.41 | 0.78 | 97.19 | 0.99 | 0.41 | 1.69 | 0.7 |
| YC4-105 | 756.7 | 98.39 | 1.04 | 99.43 | 0.99 | / | 0 | 0.57 |
| YC4-109 | 762 | 97.96 | 0.94 | 98.90 | 0.99 | 0.4 | 0 | 0.69 |
| YC4-15-1 | 655.6 | 99.36 | 0.41 | 99.77 | 1.00 | / | 0.05 | 0.18 |
| YC4-15-2 | 655.9 | 95.94 | 1.28 | 97.22 | 0.99 | / | 2.48 | 0.3 |
| YC4-15-3 | 656.2 | 99.36 | 0.49 | 99.85 | 1.00 | / | 0 | 0.15 |
| YC4-15-4 | 656.5 | 98.61 | 0.7 | 99.31 | 0.99 | / | 0 | 0.69 |
| YC4-15-5 | 656.8 | 98.34 | 1.26 | 99.60 | 0.99 | / | 0 | 0.4 |
| YC4-15-6 | 657 | 98.71 | 0.62 | 99.33 | 0.99 | / | 0 | 0.66 |
| YC4-27-1 | 667.1 | 99.32 | 0.34 | 99.66 | 1.00 | / | 0 | 0.34 |
| YC4-27-2 | 667.3 | 98.49 | 0.23 | 98.72 | 1.00 | / | 0 | 1.29 |
| YC4-27-3 | 667.5 | 95.51 | 0 | 95.51 | 1.00 | 1.81 | 0 | 2.69 |
| YC4-27-4 | 667.7 | 96.63 | 0.7 | 97.33 | 0.99 | / | 2.2 | 0.47 |
| YC4-27-5 | 667.9 | 96.87 | 0.91 | 97.78 | 0.99 | / | 1.22 | 0.99 |
| YC4-27-6 | 668.2 | 96.76 | 1.08 | 97.84 | 0.99 | 0.85 | 0 | 1.3 |

*4.3.2. Gas Molecular Composition.* In this work, a gas chromatograph equipped with a flame ionization detector and a thermal conductivity detector in used to analyze the gas molecular components, which is subsequently corrected for the bulk compositional analyses of oxygen. Herein, the statistics from 31 samples are exhibited in Table 2, where the total content of hydrocarbon gases is distributed in 95.51%~99.85%, and its average is 98.67% (therein ~0.78% belongs to $C_{6+}$), while the nonhydrocarbon gas (mainly are $CO_2$ and $N_2$) occupies small proportion (average of 0.89%). Basically, $CH_4$ is the primary composition, which occupies 95.51%~99.36% in total gas content. Besides, the content of heavy hydrocarbon gases is tiny and just has an average of 0.68%. Meanwhile, the drying coefficient has an average of 0.99, indicating the dry gas is the dominate molecular composition in the gas content of WL shale. Competitively, the drying coefficient of gases in WL shale located at different place is similar, for example, the drying coefficient is 98.58%~99.04% (98.81% on average) according to the achievements from the Well-EFD1 (E Feng Di 1) located in Xianfeng County of Hubei Province [63]. This phenomenon suggests that the $CH_4$ is dominated in the gas molecular composition for all WL shale gas in/around Sichuan basin.

## 5. Conclusions

This work exhibits a comprehensive investigation on the WL shale, represented by a shale gas exploration well in Sichuan basin, according to the drilling/logging information, petrophysical properties, and gas content. Accordingly, the main notable points yield.

The WL shale in Well-YC4 contains three third-order sequences (SS1, SS2, and SS3) from the lower section to the upper section and each sequence contains a TST and an HST. Besides, regarding SS1, SS2, and SS3, their sedimentary environment differs from each other—with different relatively oxygenic and hydrodynamics. Basically, compared to the situation of SS1 and SS2, the sediment sources in the section of SS3 seem to contain more terrigenous sand and silty materials.

The bottom section (SS1 and SS2) of WL shale has a soft great BI value than the upper section (SS3), suggesting the bottom WL shale is better suited for hydraulic fracturing than the upper section. Besides, the pore type in WL shale of Well-YC4 is diversiform, but the porosity is low; meanwhile, the high BET surface area indicates that the micropores are well developed. The TOC content and the thermal evolution degree indicate the WL shale has a decent hydrocarbon generation ability and is conducive to the full generation of shale gas. Besides, the vertical heterogeneity widely occurs to the reservoir parameters of WL shale, such as mineral composition, pore system characteristics, and organic matter.

The gas content of WL shale is 1.22 $m^3$/t in average and ranges in the scope of 0.76 $m^3$/t~2.38 $m^3$/t. In vertical, the lower section (depth of 724~736 m) has the highest gas content, compared to the middle section (685 m~724 m) and the upper section (645 m~685 m). In the total gas in WL shale, $CH_4$ is the primary composition and occupies 95.51%~99.36%, while the nonhydrocarbon gas occupies small proportion (average of 0.89%). Meanwhile, the drying coefficient averages 0.99, indicating the $CH_4$ is the dominate molecular composition in the gas content of WL shale. Basically, the gas accumulation suggests a great potential for shale gas development in the area where Well-YC4 locates at.

## Data Availability

The data used to support the findings of this study are available from the corresponding author upon request.

## Conflicts of Interest

The authors declare that the research was conducted in the absence of any commercial or financial relationships that could be construed as a potential conflict of interest.

## Acknowledgments

This study was financially supported by the Science and Technology Department of Sichuan Province (2021YFH0048), the project funded by China Postdoctoral Science Foundation (2020M683253), and the project funded by Chongqing Natural Science Foundation for Distinguished Young Scientists (cstc2021jcyj-jqX0007).

## References

[1] K. Lin, X. F. Huang, and Y. P. Zhao, "Combining image recognition and simulation to reproduce the adsorption/desorption behaviors of shale gas," *Energy & Fuels*, vol. 34, no. 1, pp. 258–269, 2020.

[2] J. Liu, L. Z. Xie, B. He, Q. Gan, and P. Zhao, "Influence of anisotropic and heterogeneous permeability coupled with in-situ stress on $CO_2$ sequestration with simultaneous enhanced gas recovery in shale: quantitative modeling and case study," *International Journal of Greenhouse Gas Control*, vol. 104, article 103208, 2021.

[3] K. Liu, L. Wang, M. Ostadhassan, J. Zou, B. Bubach, and R. Rezaee, "Nanopore structure comparison between shale oil and shale gas: examples from the Bakken and Longmaxi formations," *Petroleum Science*, vol. 16, no. 1, pp. 77–93, 2019.

[4] C. Fan, S. Li, D. Elsworth, J. Han, and Z. Yang, "Experimental investigation on dynamic strength and energy dissipation characteristics of gas outburst-prone coal," *Energy Science & Engineering*, vol. 8, no. 1-4, pp. 1015–1028, 2020.

[5] C. Fan, L. Yang, G. Wang, Q. Huang, X. Fu, and H. Wen, "Investigation on coal skeleton deformation in $CO_2$ injection enhanced $CH_4$ drainage from underground coal seam," *Frontiers in Earth Science*, vol. 9, article 766011, 2021.

[6] C. Wu, C. Yuan, G. Wen, L. Han, and H. Liu, "A dynamic evaluation technique for assessing gas output from coal seams during commingling production within a coalbed methane well: a case study from the Qinshui Basin," *International Journal of Coal Science & Technology*, vol. 7, no. 1, pp. 122–132, 2020.

[7] F. Z. Yan, J. Xu, S. J. Peng et al., "Effect of capacitance on physicochemical evolution characteristics of bituminous coal treated by high-voltage electric pulses," *Powder Technology*, vol. 367, pp. 47–55, 2020.

[8] S. H. B. Clark, F. G. Poole, and Z. C. Wang, "Comparison of some sediment-hosted, stratiform barite deposits in China, the United States, and India," *Ore Geology Reviews*, vol. 24, no. 1-2, pp. 85–101, 2004.

[9] C. N. Zou, Z. Yang, S. P. Huang et al., "Resource types, formation, distribution and prospects of coal-measure gas," *Petroleum Exploration and Development*, vol. 46, no. 3, pp. 451–462, 2019.

[10] T. Lei, Z. Wang, A. Krupnick, and X. Liu, "Stimulating shale gas development in China: a comparison with the US experience," *Energy Policy*, vol. 75, pp. 109–116, 2014.

[11] R. Liu, F. Hao, T. Engelder et al., "Stress memory extracted from shale in the vicinity of a fault zone: implications for shale-gas retention," *Marine and Petroleum Geology*, vol. 102, pp. 340–349, 2019.

[12] L. Cheng, D. Li, W. Wang, and J. Liu, "Heterogeneous transport of free CH4 and free CO2 in dual-porosity media controlled by anisotropic in situ stress during shale gas production by CO2 flooding: implications for CO2 geological storage and utilization," *ACS Omega*, vol. 6, no. 40, pp. 26756–26765, 2021.

[13] P. Zhao, L. Z. Xie, Z. C. Fan, L. Deng, and J. Liu, "Mutual interference of layer plane and natural fracture in the failure behavior of shale and the mechanism investigation," *Petroleum Science*, vol. 18, no. 2, pp. 618–640, 2021.

[14] W. E. Liss, "Impacts of shale gas advancements on natural gas utilization in the United States," *Energy Technology*, vol. 2, no. 12, pp. 953–967, 2014.

[15] G. Li, H. Liu, Y. Meng et al., "Challenges in deep shale gas drilling: a case study in Sichuan Basin," in *IADC/SPE Asia Pacific Drilling Technology Conference and Exhibition*, OnePetro, Tianjin, China, 2012.

[16] D. Dong, S. Gao, J. Huang, Q. Guan, S. Wang, and Y. Wang, "Discussion on the exploration & development prospect of shale gas in the Sichuan Basin," *Natural Gas Industry B*, vol. 2, no. 1, pp. 9–23, 2015.

[17] J. Liu, Y. Yao, D. Liu, Y. Cai, and J. Cai, "Comparison of pore fractal characteristics between marine and continental shales," *Fractals*, vol. 26, no. 2, p. 1840016, 2018.

[18] K. Wang, H. Vredenburg, T. Wang, and L. Y. Feng, "Financial return and energy return on investment analysis of oil sands, shale oil and shale gas operations," *Journal of Cleaner Production*, vol. 223, pp. 826–836, 2019.

[19] R. Liu, F. Hao, T. Engelder, Z. Zhu, and C. Teng, "Influence of tectonic exhumation on porosity of Wufeng–Longmaxi shale in the Fuling gas field of the eastern Sichuan Basin," *China. AAPG Bulletin*, vol. 104, no. 4, pp. 939–959, 2020.

[20] R. Liu, T. Wen, J. Amalberti, J. Zheng, F. Hao, and D. Jiang, "The dichotomy in noble gas signatures linked to tectonic deformation in Wufeng-Longmaxi Shale, Sichuan Basin," *Sichuan Basin. Chemical Geology*, vol. 581, article 120412, 2021.

[21] B. Xiao, L. Xiong, Z. Zhao, and X. Fu, "Sedimentary tectonic pattern of Wufeng and Longmaxi formations in the northern margin of Sichuan Basin, South China," *South China. International Geology Review*, pp. 1–20, 2021.

[22] M. An, F. Zhang, D. Elsworth, Z. Xu, Z. Chen, and L. Zhang, "Friction of Longmaxi shale gouges and implications for seismicity during hydraulic fracturing," *Journal of Geophysical Research: Solid Earth*, vol. 125, no. 8, article e2020JB019885, 2020.

[23] J. Wu, Y. Yuan, S. Niu, X. Wei, and J. Yang, "Multiscale characterization of pore structure and connectivity of Wufeng-Longmaxi shale in Sichuan Basin, China," *Marine and Petroleum Geology*, vol. 120, no. 2/3, article 104514, 2020.

[24] Z. W. Ma, G. L. Pi, X. C. Dong, and C. Chen, "The situation analysis of shale gas development in China-based on structural equation modeling," *Renewable and Sustainable Energy Reviews*, vol. 67, pp. 1300–1307, 2017.

[25] B. Figueiredo, C. F. Tsang, J. Rutqvist, and A. Niemi, "Study of hydraulic fracturing processes in shale formations with complex geological settings," *Journal of Petroleum Science and Engineering*, vol. 152, pp. 361–374, 2017.

[26] J. Liu, Y. Yao, D. Elsworth, D. Liu, Y. Cai, and L. Dong, "Vertical heterogeneity of the shale reservoir in the lower Silurian Longmaxi formation: analogy between the southeastern and northeastern Sichuan Basin, SW China," *Minerals*, vol. 7, no. 8, p. 151, 2017.

[27] H. Chen, Y. Hu, Y. Kang, X. C. A. Wang, F. Liu, and Y. W. Liu, "Advantages of supercritical $CO_2$ compound fracturing in shale on fracture geometry, complexity and width," *Journal of Natural Gas Science and Engineering*, vol. 93, article 104033, 2021.

[28] L. Hou, S. Zhang, D. Elsworth, H. L. Liu, B. J. Sun, and X. Y. Geng, "Review of fundamental studies of $CO_2$ fracturing: fracture propagation, propping and permeating," *Journal of Petroleum Science and Engineering*, vol. 205, article 108823, 2021.

[29] F. Z. Yan, J. Xu, S. J. Peng et al., "Breakdown process and fragmentation characteristics of anthracite subjected to high-voltage electrical pulses treatment," *Fuel*, vol. 275, article 117926, 2020.

[30] J. Liu, Y. Yao, D. Liu, Z. Pan, and Y. Cai, "Comparison of three key marine shale reservoirs in the southeastern margin of the Sichuan Basin, SW China," *Minerals*, vol. 7, no. 10, p. 179, 2017.

[31] R. Wang, Z. Hu, S. Long et al., "differential Characteristics of the Upper Ordovician-Lower Silurian Wufeng-Longmaxi Shale Reservoir and its implications for exploration and development of shale gas in/around the Sichuan Basin," *Acta Geologica Sinica*, vol. 93, no. 3, pp. 520–535, 2019.

[32] X. Tang, S. Jiang, Z. Jiang et al., "Heterogeneity of Paleozoic Wufeng-Longmaxi formation shale and its effects on the shale gas accumulation in the Upper Yangtze Region, China," *Fuel*, vol. 239, pp. 387–402, 2019.

[33] L. Zhang, S. Lu, S. Jiang et al., "Effect of shale lithofacies on pore structure of the Wufeng-Longmaxi shale in Southeast Chongqing, China," *Energ. Fuel*, vol. 32, no. 6, pp. 6603–6618, 2018.

[34] Z. Liu, B. Bai, J. Tang, Z. Xiang, S. Zeng, and H. Qu, "Investigation of Slickwater effect on permeability of gas shale from Longmaxi formation," *Energ. Fuel*, vol. 35, no. 4, pp. 3104–3111, 2021.

[35] X. Chen, S. Luo, J. Tan et al., "Assessing the gas potential of the lower Paleozoic shale system in the Yichang Area, Middle Yangtze Region," *Energy & Fuels*, vol. 35, no. 7, pp. 5889–5907, 2021.

[36] J. Liu, Y. Yao, D. Elsworth, Z. Pan, X. Sun, and W. Ao, "Sedimentary characteristics of the Lower Cambrian Niutitang shale in the southeast margin of Sichuan Basin, China," *Journal of Natural Gas Science and Engineering*, vol. 36, pp. 1140–1150, 2016.

[37] S. Xu, Q. Gou, F. Hao, B. Zhang, and Y. Zhang, "Multiscale faults and fractures characterization and their effects on shale gas accumulation in the Jiaoshiba area, Sichuan Basin, China," *Journal of Petroleum Science and Engineering*, vol. 189, article 107026, 2020.

[38] S. Xu, R. Liu, F. Hao et al., "Complex rotation of maximum horizontal stress in the Wufeng-Longmaxi shale on the eastern margin of the Sichuan Basin, China: implications for predicting natural fractures," *Marine and Petroleum Geology*, vol. 109, pp. 519–529, 2019.

[39] B. Xiao, S. G. Liu, Z. W. Li et al., "Geochemical characteristics of marine shale in the Wufeng Formation-Longmaxi Formation in the northern Sichuan Basin, South China and its implications for depositional controls on organic matter," *Journal of Petroleum Science and Engineering*, vol. 203, article 108618, 2021.

[40] B. Xiao, S. G. Liu, B. Ran, and Z. W. Li, "Geochemistry and sedimentology of the Upper Ordovician–lower Silurian black shale in the northern margin of the Upper Yangtze Platform, South China: implications for depositional controls on organic-matter accumulation," *Australian Journal of Earth Sciences*, vol. 67, no. 1, pp. 129–150, 2020.

[41] Z. Jiang, L. Guo, L. Chao, W. Yuan, and L. Min, "Lithofacies and sedimentary characteristics of the Silurian Longmaxi shale in the southeastern Sichuan Basin, China," *Journal of Palaeogeography*, vol. 2, no. 3, pp. 238–251, 2013.

[42] F. Hao, H. Zou, and Y. Lu, "Mechanisms of shale gas storage: implications for shale gas exploration in China," *AAPG Bulletin*, vol. 97, no. 8, pp. 1325–1346, 2013.

[43] L. Zeng, W. Lyu, J. Li et al., "Natural fractures and their influence on shale gas enrichment in Sichuan Basin, China," *Journal of Natural Gas Science Engineering*, vol. 30, pp. 1–9, 2016.

[44] J. W. Reinhardt, "Uppermost Permian reefs and Permo-Triassic sedimentary facies from the southeastern margin of Sichuan Basin, China," *Facies*, vol. 18, no. 1, pp. 231–287, 1988.

[45] J. Li, X. Wen, and C. Huang, "Lower and upper cretaceous paleosols in the western Sichuan Basin, China: implications for regional paleoclimate," *Geological Journal*, vol. 55, no. 1, pp. 390–408, 2020.

[46] L. Chen, Y. C. Lu, S. Jiang et al., "Sequence stratigraphy and its application in marine shale gas exploration: a case study of the Lower Silurian Longmaxi Formation in the Jiaoshiba shale gas field and its adjacent area in Southeast Sichuan Basin, SW China," *Journal of Natural Gas Science and Engineering*, vol. 27, pp. 410–423, 2015.

[47] Q. Y. Gou, S. Xu, F. Hao et al., "Full-scale pores and micro-fractures characterization using FE-SEM, gas adsorption, nano-CT and micro-CT: a case study of the Silurian Longmaxi Formation shale in the Fuling area, Sichuan Basin, China," *Fuel*, vol. 253, pp. 167–179, 2019.

[48] D. Fu, G. Xu, L. Ma, F. Yang, and Y. Ma, "Gas generation from coal: taking Jurassic coal in the Minhe Basin as an example," *International Journal of Coal Science & Technology*, vol. 7, no. 3, pp. 611–622, 2020.

[49] L. Chen, Y. C. Lu, S. Jiang, J. Q. Li, T. L. Guo, and C. Luo, "Heterogeneity of the Lower Silurian Longmaxi marine shale in the Southeast Sichuan Basin of China," *Marine and Petroleum Geology*, vol. 65, pp. 232–246, 2015.

[50] X. L. Tang, Z. X. Jiang, H. X. Huang et al., "Lithofacies characteristics and its effect on gas storage of the Silurian Longmaxi marine shale in the southeast Sichuan Basin, China," *Journal of Natural Gas Science and Engineering*, vol. 28, pp. 338–346, 2016.

[51] F. Y. Xiong, Z. X. Jiang, X. L. Tang et al., "Characteristics and origin of the heterogeneity of the Lower Silurian Longmaxi marine shale in southeastern Chongqing, SW China," *Journal of Natural Gas Science and Engineering*, vol. 27, pp. 1389–1399, 2015.

[52] D. M. Jarvie, R. J. Hill, T. E. Ruble, and R. M. Pollastro, "Unconventional shale-gas systems: the Mississippian Barnett shale of north-central Texas as one model for thermogenic shale-gas assessment," *AAPG Bulletin*, vol. 91, no. 4, pp. 475–499, 2007.

[53] Y. Li and J. Cai, "Effect of semectite illitization on shale gas occurrence in argillaceous source rock," *Petroleum Geology & Experiment*, vol. 36, no. 3, pp. 346–352, 2014.

[54] J. Liu, Y. Yao, Z. Zhu, L. Cheng, and G. Wang, "Experimental investigation of reservoir characteristics of the upper Ordovician Wufeng Formation shale in middle–upper Yangtze region, China," *Energy Exploration & Exploitation*, vol. 34, no. 4, pp. 527–542, 2016.

[55] S. Xu, Q. Gou, F. Hao et al., "Shale pore structure characteristics of the high and low productivity wells, Jiaoshiba shale gas field, Sichuan Basin, China: dominated by lithofacies or preservation condition?," *Marine and Petroleum Geology*, vol. 114, article 104211, 2020.

[56] T. Lin, X. Liu, J. Zhang et al., "Characterization of multi-component and multi-phase fluids in the Upper Cretaceous oil shale from the Songliao basin (NE China) using T1–T2NMR correlation maps," *Petroleum Science and Technology*, vol. 39, no. 23-24, pp. 1060–1070, 2021.

[57] P. Hou, X. Liang, F. Gao, J. Dong, and Y. Xue, "Quantitative visualization and characteristics of gas flow in 3D pore-fracture system of tight rock based on lattice Boltzmann simulation," *Journal of Natural Gas Science and Engineering*, vol. 89, no. 4, article 103867, 2021.

[58] P. Hou, X. Liang, Y. Zhang, J. He, F. Gao, and J. Liu, "3D multi-scale reconstruction of fractured shale and influence of fracture morphology on shale gas flow," *Natural Resources Research*, vol. 30, no. 3, pp. 2463–2481, 2021.

[59] F. Z. Yan, J. Xu, B. Q. Lin, S. J. Peng, Q. L. Zou, and X. L. Zhang, "Changes in pore structure and permeability of anthracite coal before and after high-voltage electrical pulses treatment," *Powder Technology*, vol. 343, pp. 560–567, 2019.

[60] P. Hou, S. J. Su, X. Liang et al., "Effect of liquid nitrogen freeze-thaw cycle on fracture toughness and energy release rate of saturated sandstone," *Engineering Fracture Mechanics*, vol. 258, article 108066, 2021.

[61] X. Liang, P. Hou, Y. Xue, X. Yang, F. Gao, and J. Liu, "A fractal perspective on fracture initiation and propagation of reservoir rocks under water and nitrogen fracturing," *Fractals*, vol. 29, no. 7, 2021.

[62] R. Hartman, R. Ambrose, and I. Akkutlu, "Shale gas-in-place calculations part II - multicomponent gas adsorption," in *Proceeding of SPE Unconventional Gas Conference*, pp. 14-15, Woodlands, TX, June 2011.

[63] S. Z. Li, F. Y. Meng, X. T. Zhang et al., "Gas composition and carbon isotopic variation during shale gas desorption: implication from the Ordovician Wufeng Formation-Silurian Longmaxi Formation in west Hubei, China," *Journal of Natural Gas Science and Engineering*, vol. 87, article 103777, 2021.